

# Investigating the Influence of Porosity on Thermal and Mechanical Properties of a C/C Composite Using Image Based FE Modelling

Abdulrahman A. Alghamdi, Paul M. Mummery, Mohammad A. Sheikh

**Abstract**—In this paper, 3D image based composite unit cell is constructed from high resolution tomographic images. Through-thickness thermal diffusivity and in-plane Young's modulus are predicted for the composite unit cell. The accuracy of the image based composite unit cell is tested by comparing its results with the experimental results obtained from laser flash and tensile test. The FE predictions are in close agreement with experimental results. Through-thickness thermal diffusivity and in-plane Young's modulus of a virgin C/C composite are predicted by replacing the properties of air (porosity) with the properties of carbon matrix. The effect of porosity was found to be more profound on thermal diffusivity than young's modulus.

**Keywords**—Porosity, C/C composite, image based FE modelling, CMC.

## I. INTRODUCTION

It is well established that the presence of manufacturing porosity in ceramic matrix composites (CMCs) has a direct effect on their thermal and mechanical properties. As a result, it is essential to predict thermal and mechanical properties of CMCs at an early stage in the design process [1]. Unfortunately, due to lack of homogeneity in woven fibre reinforced composites, it is not always possible to calculate the equivalent thermal and mechanical properties of such materials by using a specific set of equations such as the rule of mixture. For such materials with complex architectures, finite element method has been employed with a high degree of reliability and accuracy. This has led to a reduction in the amount of experimental work and hence the design and development costs. However, the geometrical complexity of the manufacturing porosity makes it impossible to be modelled. Due to that, the image based modelling technique, which allows a detailed 3-D model of a specimen to be created from high resolution tomographic images, has been used in this study.

In this work, the thermal and mechanical behaviour (with and without porosity) of a 2D C/C composite is investigated

A. Alghamdi is a PhD candidate at the University of Manchester, School of Mechanical, Aerospace and Civil Engineering, M13 9PL, Manchester, UK (phone: 00447412622304; e-mail: abdulrahman.alghamdi-2@postgrad.manchester.ac.uk).

P. Mummery is with the University of Manchester, School of Mechanical, Aerospace and Civil Engineering, M13 9PL, Manchester, UK ( e-mail: paul.m.mummery@manchester.ac.uk).

M. Sheikh is with the University of Manchester, School of Mechanical, Aerospace and Civil Engineering, M13 9PL, Manchester, UK (phone: 0044(0)161-306-3802; e-mail: mohammad.a.sheikh@manchester.ac.uk).

using the image based finite element modelling technique. The real macro-structures of the composite, directionality of the carbon tows, and the presence of different phases, including all types of porosity, are taken into account by converting tomographic images to a detailed 3D finite element model of the composite unit cell.

## II. EXPERIMENTAL SET UP

### A. Material under Investigation

A carbon matrix composite reinforced with polyacrylonitrile (PAN) carbon fibres was provided by the XingheMuzi Carbon Co. [2] for use within this study. This composite was fabricated from ten layers of a 2D 2/2 twill weave cloth, using the liquid impregnation technique. The principle of this technique is to infiltrate the reinforcement preform with liquid polymeric resin, followed by pyrolysis to convert the resin into carbon matrix. Further cycles of impregnation are then used to densify the composite. Finally, the composite is carbonised by heating to 2300°C.

### B. X-ray Tomography

A Nikon Metris Custom Bay laboratory X-ray micro-tomography instrument was used to acquire raw 3D tomographic data on the C/C composite. In X-ray micro-tomography, the specimen is irradiated with an X-ray beam and the reduction in X-ray intensity measured after transmission through the sample. Some of the X-ray photons are absorbed by the sample, while the remainder pass through the specimen and are measured by the detector. A series of projections at different angular rotations from 0° to 360° were taken to acquire a 3D representation of the composite.

### C. Laser Flash Test

The through-thickness thermal diffusivity of the C/C composite was measured by using a laser flash system (Model LFA 457, NETZSCH Group, Germany). This technique was first proposed by Parker et al. [3]. It works on the principle of applying a laser pulse on the entire front face of a disc specimen for few milliseconds, and recording the temperature changes as a function of time on the opposite face of the test piece. From the recorded data the required time to reach the temperature equivalent to half of the maximum temperature, which is called the half rise time ( $t_{1/2}$ ), is obtained. Thermal diffusivity is then calculated as follows:

$$\alpha = 0.1388L^2/t_{1/2} \quad (1)$$

where  $\alpha$  is thermal diffusivity,  $L$  is the sample (disc) thickness.

#### D. Tensile Test

Young's modulus of the examined C/C composite was measured on a tensile testing machine (Model 4507, INSTRON Corporation, USA). Tensile tests were performed according to the standard for tensile testing of continuous fibre-reinforced ceramic composites (CFCC) at ambient temperature ASTM C 1275[4].

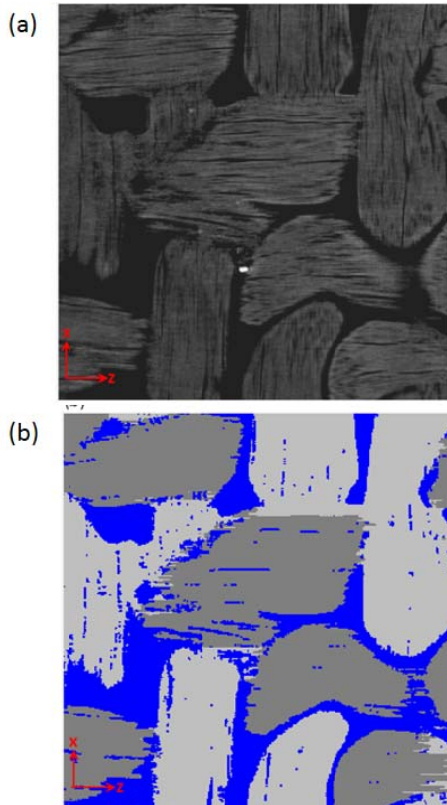


Fig. 1 Tomographic image of the composite (a) before and (b) after segmentation; blue = porosity, dark grey = warp tows, light grey = fill tows

### III. FINITE ELEMENT MODELLING

#### A. Image Based Modelling

The resulting tomographic images of the C/C composite were imported to Scan IP software [5] for segmentation process where different phases of the composite (porosity, longitudinal and transverse fibre tow) were separated. The different phases in the stacked images can be distinguished by a naked eye, as shown in Fig. 1 (a), but it is still difficult for these phases to be separated by the software using the grey-scale, as the longitudinal and transverse fibre tows have the same absorption coefficient and therefore the same grey level. Due to this a manual segmentation process was carried out for the construction of the composite unit cell as shown in Fig. 1 (b). The volume fractions of warp tows, fill tows and porosity are 0.4, 0.413 and 0.186 respectively. The volume of the unit

cell is  $5.08 \times 0.51 \times 5.15 \text{ mm}^3$ . Fig. 2 (a) shows the 3D image based composite unit cell. Scan IP was then used to create a detailed finite element mesh of the carbon-carbon composite. The mesh obtained has a combination of 10,457,324 tetrahedral elements and 2,043,817 hexahedral elements as shown in Fig. 2 (b). The final finite element mesh was then exported to ABAQUS FE package for thermal and mechanical analyses. The material properties applied to each phase are listed in Table I.

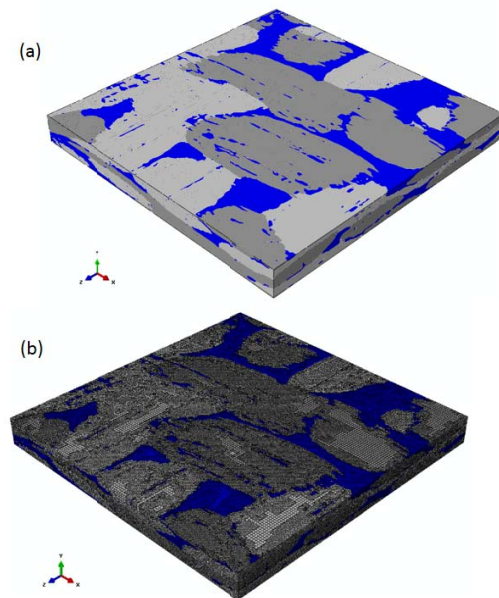


Fig. 2 (a) Image based composite unit cell and its (b) FE mesh

TABLE I  
MATERIAL PROPERTIES OF THE CONSTITUENT MATERIALS [6]-[9]

	K (W/m-K)	$C_p$ (J/kg-K)	$\rho$ (kg/m <sup>3</sup> )	E (GPa)	$\nu$
Carbon Tow	8.2 (//) 2.6(⊥)	1038.8	1317	20.9(//) 8.5(⊥)	0.2
Carbon Matrix	6.3	1256	1400	11.4	0.2
Air	0.026	1000	1.3	--	--

#### B. Thermal Analysis

The laser flash test was simulated by transient thermal analysis which involves applying surface heat flux on the top face of the composite unit cell for two milliseconds and recording the temperature changes as a function of time on the back surface, while the surrounding faces are thermally insulated, as shown in Fig. 3. From the temperature history, the time to reach the temperature equal to half of the maximum average temperature, the half rise time ( $t_{1/2}$ ), is obtained. The through thickness thermal diffusivity is then calculated by using (1).

#### C. Mechanical Analysis

The boundary conditions for the mechanical analysis of the composite unit cell were set to simulate the tensile test by applying a specific displacement (0.5mm/min) at the right face

while the left face is fixed, as shown in Fig. 4. Young's modulus was then calculated from the stress-strain curve which was obtained by averaging the stresses and at the nodes on the central plane between the fixed and displaced faces.

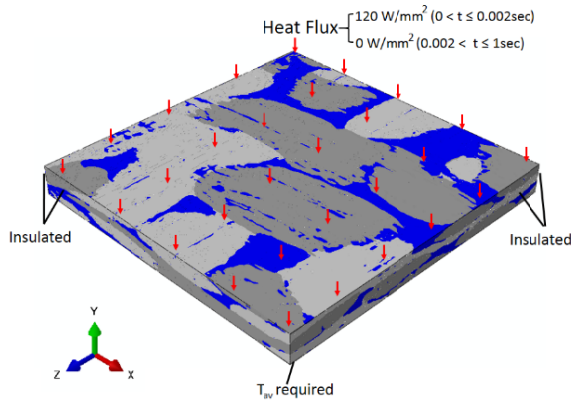


Fig. 3 Thermal boundary conditions

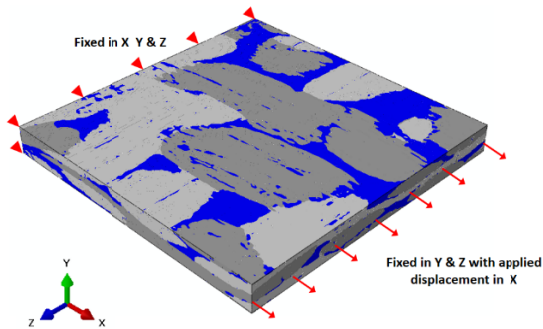


Fig. 4 Mechanical boundary conditions

#### IV. RESULTS AND DISCUSSION

##### A. Experimental Results

The average experimental values of through-thickness thermal diffusivity and in-plane Young's modulus of the composite were obtained from the laser flash and tensile tests. The mean of values of thermal diffusivity and Young's modulus were found to be  $0.709 \text{ mm}^2/\text{sec}$  and  $10.73 \text{ GPa}$  respectively. These values were taken as reference values to validate the finite element predictions.

##### B. Finite Element Results

Transient thermal analysis was carried out on the composite unit cell in y-direction to predict the through-thickness thermal diffusivity. As described earlier, thermal diffusivity calculations require the measurement of average temperature as a function of time on the bottom face of the composite unit cell. This was achieved by creating a single node set containing all the nodes on the bottom face. ABAQUS software was used to calculate the average temperature for the node set every one microsecond time step for one second. By obtaining half rise time ( $t_{1/2}$ ) from the temperature profile, the

thermal diffusivity was calculated by using (1) and was found to be  $0.672 \text{ mm}^2/\text{Sec}$ , given in Table II. This value is 5.2% lower than the average experimental value obtained by the laser flash tests.

The mechanical analysis of the composite unit cell was carried out in the two (x and z) in-plane directions. Young's moduli were found to be  $11.5 \text{ GPa}$  and  $9.54 \text{ GPa}$  in x and z directions respectively. An average value of  $10.52 \text{ GPa}$  was taken for comparison with the average experimental value of  $10.732 \text{ GPa}$  which is 2% lower (Table II).

TABLE II  
COMPARISON OF THE FE RESULTS WITH THE EXPERIMENTAL RESULTS

Property	Unit	Experimental	FEM
Thermal diffusivity	$\text{mm}^2/\text{sec}$	0.709	0.672
Young's Modulus	GPa	10.73	10.52

Hence the composite image based unit cell showed excellent results compared to the experimental results; it was used here to investigate the influence of porosity on thermal diffusivity and Young's modulus of the composite. In order to predict the thermal diffusivity and Young's modulus of a virgin C/C composite, it was assumed that the composite was perfectly densified and all the porosity areas were filled with carbon matrix. Transient thermal analysis was carried out on the image based composite unit cell, which was used before, with replacing the properties of air (porosity) with the carbon matrix properties. Fig. 5 shows the temperature profile on the bottom face of the image based composite unit cell with and without porosity. The predicted through-thickness thermal diffusivity of the virgin composite was found to be  $0.926 \text{ mm}^2/\text{sec}$ . The thermal diffusivity of the real composite unit cell (with porosity) was found previously to be  $0.672 \text{ mm}^2/\text{sec}$ . From these two values the degradation of thermal diffusivity due to porosity was found to be 27.4%.

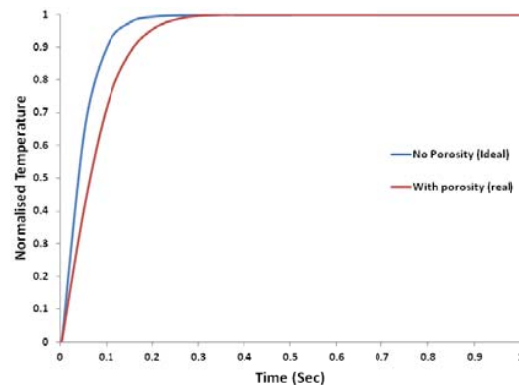


Fig. 5 Temperature profile on the bottom face of the composite unit cell with and without porosity

Similar to the thermal analysis, steady-state mechanical analysis was carried out on the image based composite unit cell, which was used before, with replacing the properties of air (porosity) with the carbon matrix properties. Fig. 6 shows the stress-strain response of the image based composite unit cell with and without porosity. The predicted value of

Young's modulus of the virgin composite (without porosity) was found to be 12.9 GPa. The effect of porosity can be determined by comparing this value with the value predicted before, which is 10.73 GPa. It was found that porosity caused 16.8% reduction in in-plane Young's modulus.

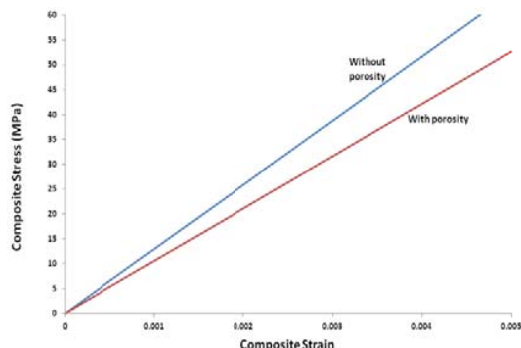


Fig. 6 Stress- strain curve of the composite unit cell with and without porosity

## V. CONCLUSION

Various steady-state and transient mechanical and thermal analyses have been carried out image based composite unit cell constructed from high resolution tomographic images in attempt to investigate the effect of manufacturing porosities on the degradation of in-plane Young's modulus and through-thickness thermal diffusivity of C/C composite. From the output results it was found that, the manufacturing porosity has more profound effect on thermal diffusivity than young's modulus.

## REFERENCES

- [1] D. Puglia, M. Sheikh, and D. Hayhurst, "Thermal transport property prediction of a CMC laminate from base materials properties and manufacturing porosities," *Proceedings of The Royal Society A*, vol. 461, pp. 3575-3597, 2005.
- [2] Xinghe Muzi Carbon Company, China.
- [3] W.J. Parker, R. J. Jenkins, C. P. Butler and G. L. Abbott "Flash method of determining thermal diffusivity, heat capacity and thermal conductivity," *Journal of Applied Physics*, vol. 32, pp. 1679-1684, 1961.
- [4] ASTM, C1275-00 "Standard Test Method For Monotonic Tensile Behaviour Of Continuous Fiber-Reinforced Advanced Ceramics With Solid Rectangular Cross-Section Test Specimens At Ambient Temperature," ASTM International, West Conshohocken, PA, 2000, [www.astm.org](http://www.astm.org).
- [5] Scan IP, [www.simpleware.co.uk](http://www.simpleware.co.uk). 2010.
- [6] A. Alghamdi, P. Mummery and M. Sheikh, "Multi-scale 3D image based modelling of carbon/carbon composite," *Journal of Modelling and Simulation in Materials Science and Engineering*, submitted for publication.
- [7] Tomkova B, Sejnoha M, Novak J and Zeman J 2008 Evaluation of effective thermal conductivities of porous textile composites *Journal of multiscale modelling* 6(2):153-67.
- [8] Ali J and Mummery P 2006 Image based modelling of carbon carbon composites *energy materials*. 1(3):179-86.
- [9] Lemmon EW and Jacobsen RT 2004 Viscosity and thermal conductivity equations for Nitrogen, Oxygen, Argon, and Air *Int. J. Thermophys.* 25(1):21-69.